


Article

Atomistic Modeling of Various Doped Mg_2NiH_4 as Conversion Electrode Materials for Lithium Storage

Zhao Qian ^{1,*}, Guanzhong Jiang ¹ , Yingying Ren ¹, Xi Nie ¹ and Rajeev Ahuja ²

¹ Key Laboratory for Liquid-Solid Structural Evolution and Processing of Materials (Ministry of Education), Shandong University & Shenzhen Institute of Shandong University, Shenzhen 518057, China; jiangguanzhongsdu@163.com (G.J.); llhjyqjyb@163.com (Y.R.); 17861412028@139.com (X.N.)

² Condensed Matter Theory Group, Department of Physics and Astronomy, Ångström Laboratory, Uppsala University, SE-75237 Uppsala, Sweden; rajeev.ahuja@physics.uu.se

* Correspondence: qianzhao@sdu.edu.cn

Received: 16 April 2019; Accepted: 15 May 2019; Published: 17 May 2019



Abstract: In this work, we have compared the potential applications of nine different elements doped Mg_2NiH_4 as conversion-type electrode materials in Li-ion batteries by means of state-of-the-art Density functional theory calculations. The electrochemical properties, such as specific capacity, volume change and average voltage, as well as the atomic and electronic structures of different doped systems have been investigated. The Na doping can improve the electrochemical capacity of the pristine material. Si and Ti doping can reduce the band gap and benefit the electronic conductivity of electrode materials. All of the nine doping elements can help to reduce the average voltage of negative electrodes and lead to reasonable volume changes. According to the computational screening, the Na, Si and Ti doping elements are thought to be promising to enhance the comprehensive properties of pure material. This theoretical study is proposed to encourage and expedite the development of metal-hydrides based lithium-storage materials.

Keywords: conversion electrode materials; doping; metal hydrides; lithium storage; first-principles

1. Introduction

Fossil fuels are being increasingly replaced by clean energies because of the pollution problems caused by the burning of traditional energy forms [1–3]. New types of energies are significant to be developed and applied in industry, as well as daily life. In this context, the renewable energy issue has become a hot topic and is absorbing more and more attention of scientists throughout the world [4,5]. In recent years, various renewable energies have been rapidly developed. Hydrogen, as a kind of energy carrier instead of energy source, is considered to be promising if abundant hydrogen can be produced using electrolysis or photocatalytic water splitting or chemical reforming. While the application of this energy form encounters some bottlenecks, such as the difficulty in solid-state hydrogen storage. This issue was interestingly defused by Aymard et al. to link metal hydrides with Li-ion battery technology and pave a new way to utilize hydrides materials in renewable energy storage [6–9].

Li-ion battery is regarded as one promising device in electric vehicles and other industrial systems [10,11]. In order to satisfy the demands of the future market, more studies need to be carried out to improve the performance of Li-ion batteries. Beyond the traditional intercalation-type and alloying-type electrodes, the electrochemical conversion reaction electrode is another kind of concept that is more tolerant of the size of ions (Li^+ , Na^+ , K^+ , etc.) and the crystal structure of electrode materials. Oumellal et al. had proposed a new type of electrode material, i.e., metal hydrides, such as MgH_2 for the conversion-type negative electrode application in Li-ion batteries. The proposed MgH_2 electrode shows a large, reversible capacity of 1480 mAhg^{-1} at an average voltage of 0.5V versus

Li^+/Li^0 which is suitable for the negative electrode [12]. The adoption of conversion electrodes has attracted more and more attention of scientists throughout the world. The pioneering conversion reaction driven by MgH_2 and Li brought new light for the application of metal hydrides for energy storage in the future.

Mg_2NiH_4 is a kind of hydride traditionally studied as hydrogen storage material to store energy in the H-host bonds. Its high hydrogen storage capacity and stable crystal structure attracted researchers' attention and the investigations on Mg_2NiH_4 have grown rapidly [13–21]. While in this work, we have explored its potential usage as the conversion electrode material to improve its electrochemical properties for lithium storage. Doping is an effective method in materials science to improve the performance of matters. In this work, a variety of elements which are close to Mg (Al, Ca, K, Na, Si) or Ni (Fe, Co, Ti, Mn) in the periodic table have been doped in Mg_2NiH_4 . Through First-principles theory, the effects of the dopants on atomic and electronic structures have been calculated. The volume change, average voltage and electrochemical capacity are further calculated.

2. Methods

All the calculations, including the atomic structures, energies, properties and electronic density of states are based on the Density functional theory (DFT) [22] and the projector augmented wave (PAW) [23] method was chosen. The Vienna Ab-initio Simulation Package was applied in this work. The scheme of Perdew-Burke-Ernzerhof (PBE) [24] in the generalized gradient approximation (GGA) was used as the exchange correlation functional. The unit cell of the $\text{Mg}_{16}\text{Ni}_8\text{H}_{32}$ (space group C2/c) owns 56 atoms with the lattice parameters $a = 14.2647 \text{ \AA}$, $b = 6.3583 \text{ \AA}$, $c = 6.4379 \text{ \AA}$ and the energy cut off was chosen as 520 eV in all calculations process. As for the Ni element, the spin polarized calculations were taken into consideration. The k-points mesh of $7 \times 15 \times 15$ was used in calculations. Geometry optimizations and structural relaxations have been done by minimizing the forces on atoms with a conjugate gradient algorithm and meanwhile minimizing stresses on unit cells without any symmetry constraint.

3. Results and Discussion

Figure 1 shows the basic structure of the $\text{Mg}_{16}\text{Ni}_8\text{H}_{32}$ crystal with the space group C2/c which has been relaxed using density functional theory calculations. According to the results of calculation, the unit cell contains 56 atoms (16 Mg atoms, 8 Ni atoms and 32 H atoms). All of the atoms include the Mg atoms with 3 different kinds of site occupancies, the Ni atoms with one kind of site occupancy and the H atoms with 4 different kinds of site occupancies. The 3 kinds of Mg atoms are named from Mg1 to Mg3 and the H atoms are named from H1 to H4. The atomic positions are shown in Table 1. The doping calculations afterwards are based on this pristine structure.

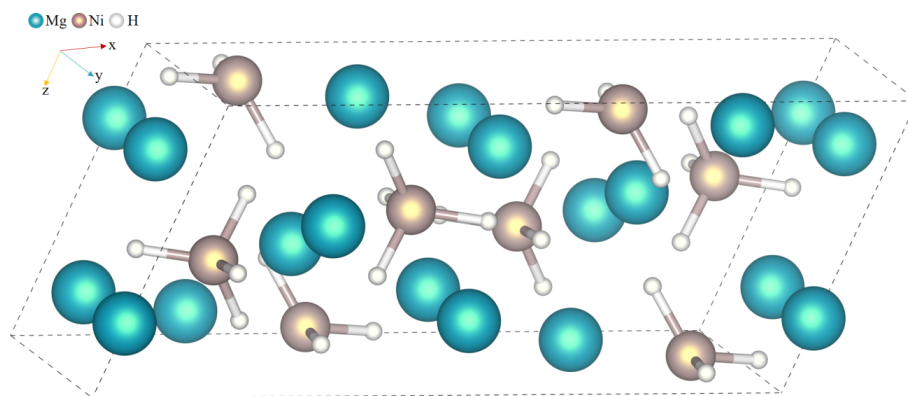


Figure 1. The unit cell of Mg_2NiH_4 . Mg atoms are shown in cyan, Ni atoms are in brown and H atoms are in white colors.

Table 1. Atomic positions in Mg_2NiH_4 .

Atom Type	Site	x	y	z
Mg1	8f	0.26389	0.48813	0.08155
Mg2	4e	0.00000	0.02287	0.25000
Mg3	4e	0.00000	0.52380	0.25000
Ni	8f	0.11991	0.23067	0.07987
H1	8f	0.21074	0.30420	0.30318
H2	8f	0.13847	0.31959	0.87295
H3	8f	0.00890	0.28864	0.05115
H4	8f	0.12497	0.98652	0.07292

In this work, nine kinds of elements that are close to Mg or Ni in the periodic table are chosen to dope into the $\text{Mg}_{16}\text{Ni}_8\text{H}_{32}$, as shown in Table 2. All the four different sites of Mg and Ni in a pristine structure are considered when doping using each kind of foreign elements. The formation energy can represent the thermodynamic doping tendency and it is calculated by the following formula [25,26]:

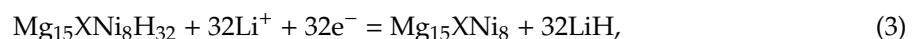
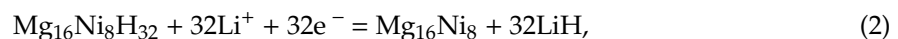
$$E_{\text{form}} = E_{\text{T}}(\text{D}) + \mu_{\text{h}} - E_{\text{T}}(\text{P}) - \mu_{\text{d}}, \quad (1)$$

where μ_{h} and μ_{d} stand for the atomic potentials of the host and dopant atoms, $E_{\text{T}}(\text{P})$ and $E_{\text{T}}(\text{D})$ stands for the total energies of pure $\text{Mg}_{16}\text{Ni}_8\text{H}_{32}$ and doped $\text{Mg}_{16}\text{Ni}_8\text{H}_{32}$. The results are listed in Table 2. It is obvious that most doping atoms prefer to replace the Mg site(s) rather than the Ni site. As for each doping system, there also exists a difference in formation of energy between different kinds of Mg sites. The Na, K, and Ca atoms prefer to replace the Mg1 site. Al and Si atoms tend to occupy the Mg2 site. Ti, Mn, Fe and Co atoms will substitute the Mg3 site. These calculations help to confirm the doped structure and lay important foundations for the further calculations of electrochemical properties for lithium storage.

Table 2. The calculated formation energies (eV) of different doping atoms and sites for Mg_2NiH_4 .

Element	Mg1 Site	Mg2 Site	Mg3 Site	Ni Site
Na	0.18689	0.19680	0.20369	0.88411
Al	−0.05240	−0.08164	−0.04217	0.59143
Si	−0.09707	−0.12752	−0.04054	0.43428
K	0.29441	0.37751	7.66576	0.97687
Ca	−0.12695	−0.11233	−0.12014	0.72187
Ti	−0.33983	−0.32535	−0.34227	0.30145
Mn	−0.12189	−0.11608	−0.12628	0.39103
Fe	−0.17242	−0.15257	−0.19421	0.14697
Co	−0.15074	−0.13761	−0.16507	0.05557

The following reactions are considered when pure and various doped Mg_2NiH_4 are respectively used as the conversion-type electrode material:



In the reactions, X represents the respective doping atom. As for the electrode material, the theoretical electrochemical capacity is one of the most important parameters to weigh the ability of the electrode. According to Faraday's law,

$$\text{The specific capacity} = nF/3600M, \quad (4)$$

where n is the number of electrons involved in the conversion reaction, F is the Faraday constant and M means the molar weight of the unit cell. Based on the doped structures, the electrochemical capacities of various systems are shown in Figure 2. It can be found that the Na doped material owns the highest electrochemical specific capacity. Besides the electrochemical capacity, the volume change of electrode materials through the conversion reaction is also an important property. In Figure 3, the Na and K dopings have the smallest volume changes (8.66% and 8.48% respectively). The volume changes of most of the doped electrode materials are less than 10%.

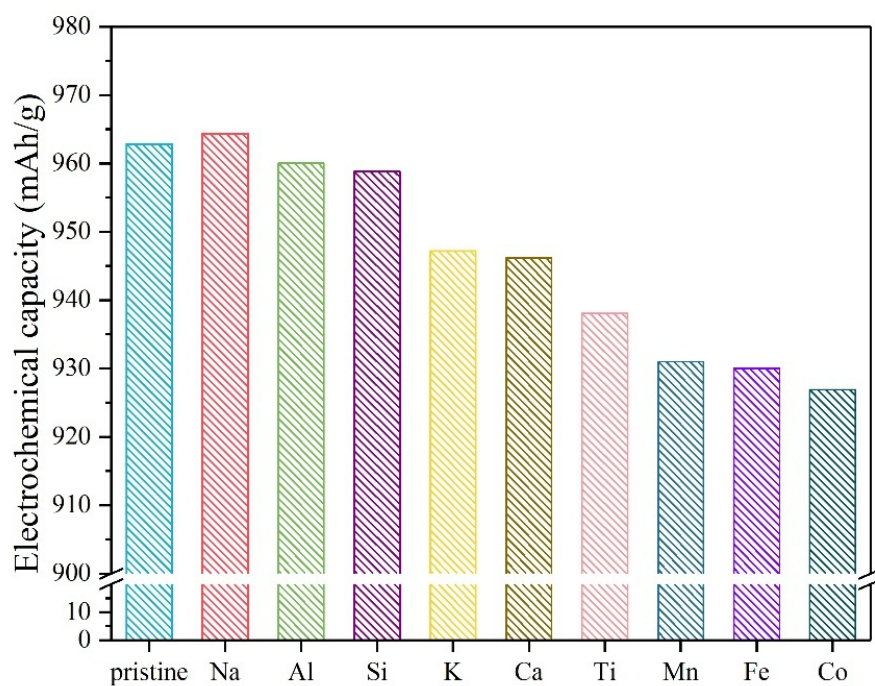


Figure 2. The specific capacity comparison of pristine and various doped Mg_2NiH_4 .

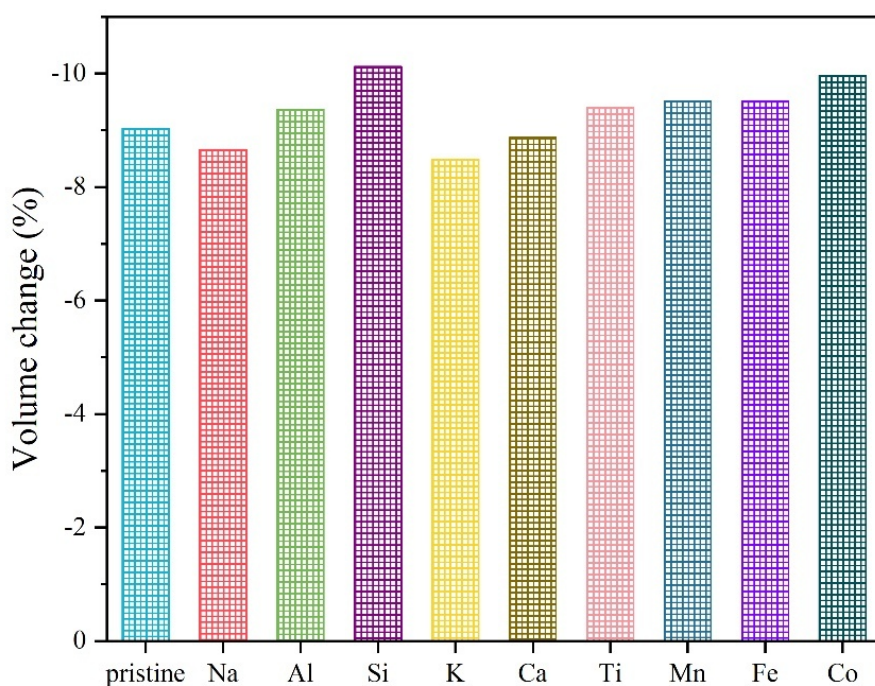


Figure 3. The volume changes of pristine and various doped Mg_2NiH_4 electrode materials.

For a good candidate for electrode material, the average voltage is another important property. According to the earlier method:

$$\text{The average voltage } V \approx -\Delta G/32F, \quad (5)$$

the average voltage values have been calculated [27,28]. In the formula, ΔG is the Gibbs free energy of the electrode conversion reaction in (2) or (3), and F is the Faraday constant. In Figure 4, it can be found that all the doping elements can reduce the average voltage of the pristine material, which is beneficial for the application as a negative electrode. The average voltage of the Mn-doped system is the lowest and the Ti-doped and Fe-doped materials follow it. The dopant of Na can reduce the average voltage to 0.467 V from the pristine 0.537 V. Considering the high capacity of the Na-doped system, this element is also acceptable as the dopant. Besides the above properties, the electronic band gap of the material should also be considered, since it is closely related to the electronic conductivity of the electrode. The comparison of various systems is shown in Figure 5. Among them, the dopants of Si and Ti have the most obvious effects to reduce the electronic band gap of the electrode material.

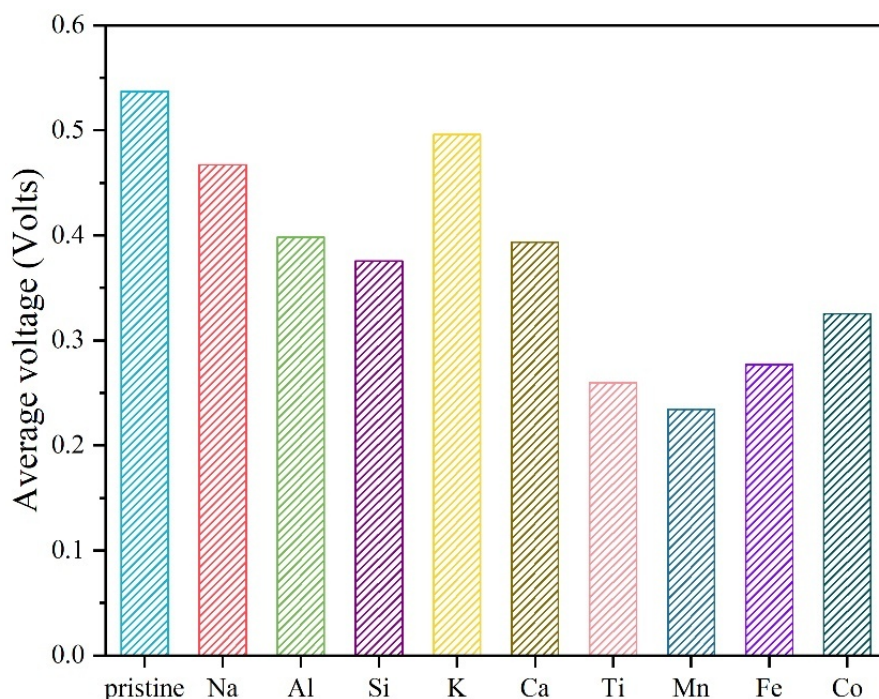


Figure 4. The average voltages of pristine and various doped Mg_2NiH_4 electrode materials.

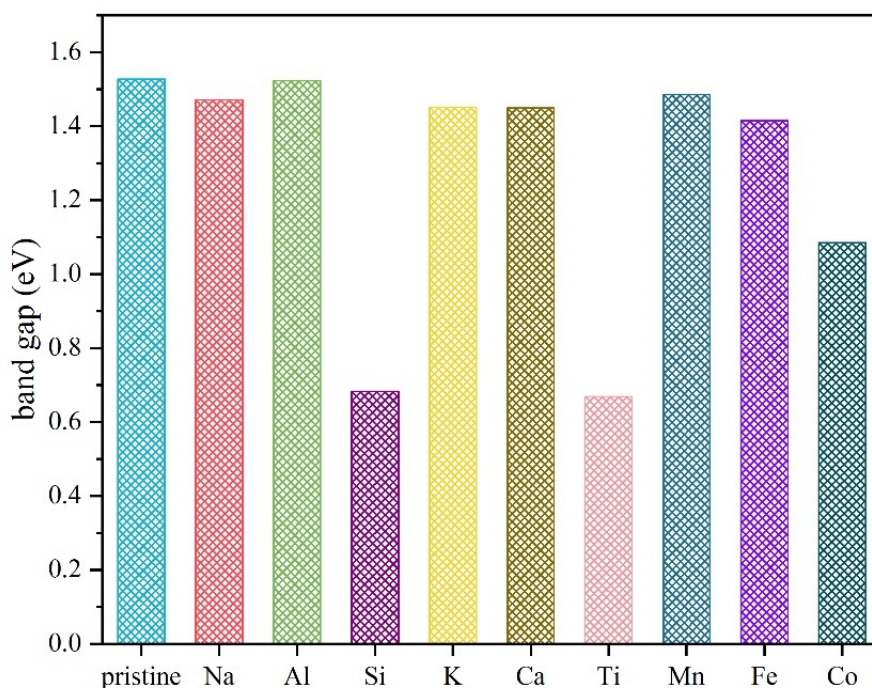


Figure 5. The electronic band gap of pristine and various doped Mg_2NiH_4 .

Through comparisons of above comprehensive electrochemical properties of various metal doped Mg_2NiH_4 systems for lithium-storage negative electrodes applications, it is found that the Na-doped material owns the highest electrochemical specific capacity while with the second smallest volume change (i.e., with good volumetric stability, which is significant for cycling properties of electrode materials concerning conversion reactions during the working process of batteries) and the reasonably low average voltage and band gap values (closely related to the electronic conductivity and rate capability of electrode materials). The Ti-doped system has the smallest electronic band gap, the second lowest average voltage as a negative electrode and the acceptable specific capacity and volume change. Besides the Na and Ti doping, the Si-doped system is also well balanced in electrochemical properties in terms of the electronic band gap, electrode average voltage, volume change and the specific capacity, which makes it another good candidate for potential conversion-type negative electrode applications. Apart from the electrochemical properties point of view, these three elements are also abundant, which further makes them regarded as the promising dopants to improve the conversion-type lithium storage properties of pristine Mg_2NiH_4 .

To reveal the underlying atomic and electronic structures of these doped materials, we have examined these systems carefully. Figure 6 shows the most stable structures after relaxations of doped Mg_2NiH_4 by Na, Si and Ti respectively. According to the above formation energy calculations, these three doping elements occupy three different sites of Mg in a crystal lattice. Figures 7–9 respectively shows the total and partial electronic density of states of three doped systems. Figure 7 shows the DOS of the Na-doped material. The total DOS curve can be divided into three parts: The part below -2.5 eV, the part from -2.5 eV to 0 eV (top of the valence band) and the part above 1.47 eV (conduction band). The electronic DOS near the Fermi energy level is mainly contributed by the Mg p-states and the Ni d-states. The partial DOS can be used to analyze chemical bonding. The s-states of Mg1, Mg2 and Mg3 tend to overlap the d-state of Ni. The p-state of Na tends to overlap the p-state of Mg. Figure 8 shows the total and partial DOS of the Si-doped material. The total DOS is also divided into three parts: From -12.5 eV to -4.2 eV; from -3.45 eV to 0 eV (top of the valence band); and the part above 0.68 eV (conduction band). When it comes to the partial DOS, the situation is similar to the Na-doped structure. The d-state of Ni atom forms bonding with the s-states of Mg atoms. What's more, the p-state of Si atom will form bonding with the p-state of Mg atom. Figure 9 shows the total and partial DOS of the

Ti-doped system. For the Ti atom, the d-state overlaps the p-state of the Mg2 atom. The common characteristics of the three doped systems are that one Ni atom would attract four H atoms to form a local structure and the Mg atom attracts Ni to be arranged around the local structure.

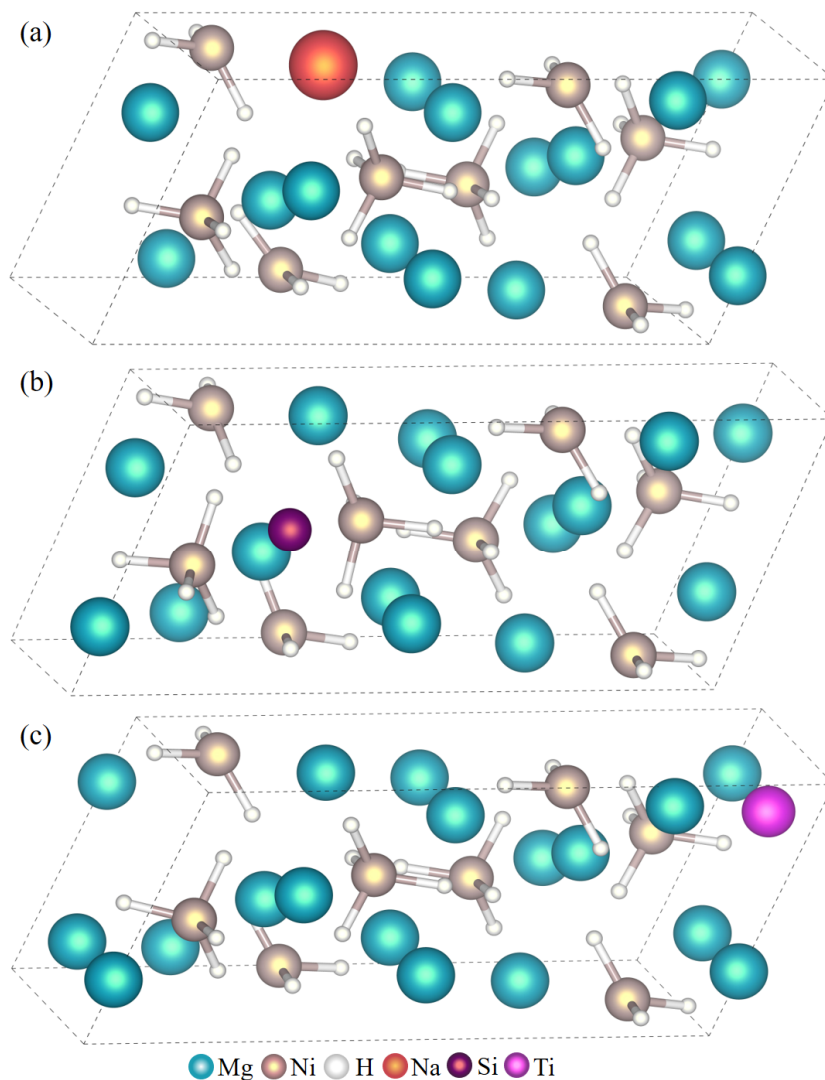


Figure 6. (a) stands for the Na doped Mg_2NiH_4 , (b) stands for the Si doped Mg_2NiH_4 , (c) stands for the Ti doped Mg_2NiH_4 . The atomic configurations of most thermodynamically stable doped Mg_2NiH_4 respectively with Na, Si and Ti: Na dopes Mg1 site, Si dopes Mg2 site and Ti dopes Mg3 site.

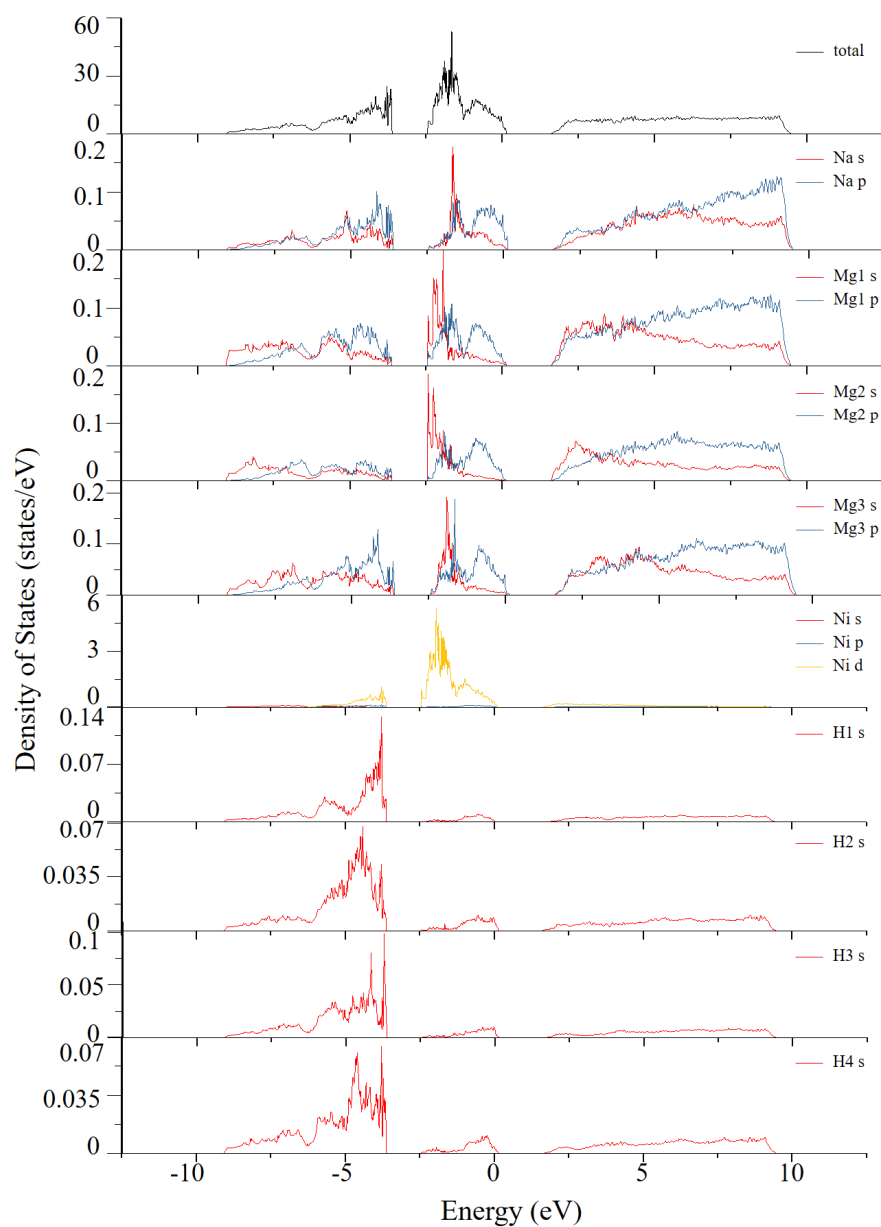


Figure 7. The calculated total and partial electronic density of states (DOS) for the Na-doped Mg_2NiH_4 solid. The Fermi level is set at zero.

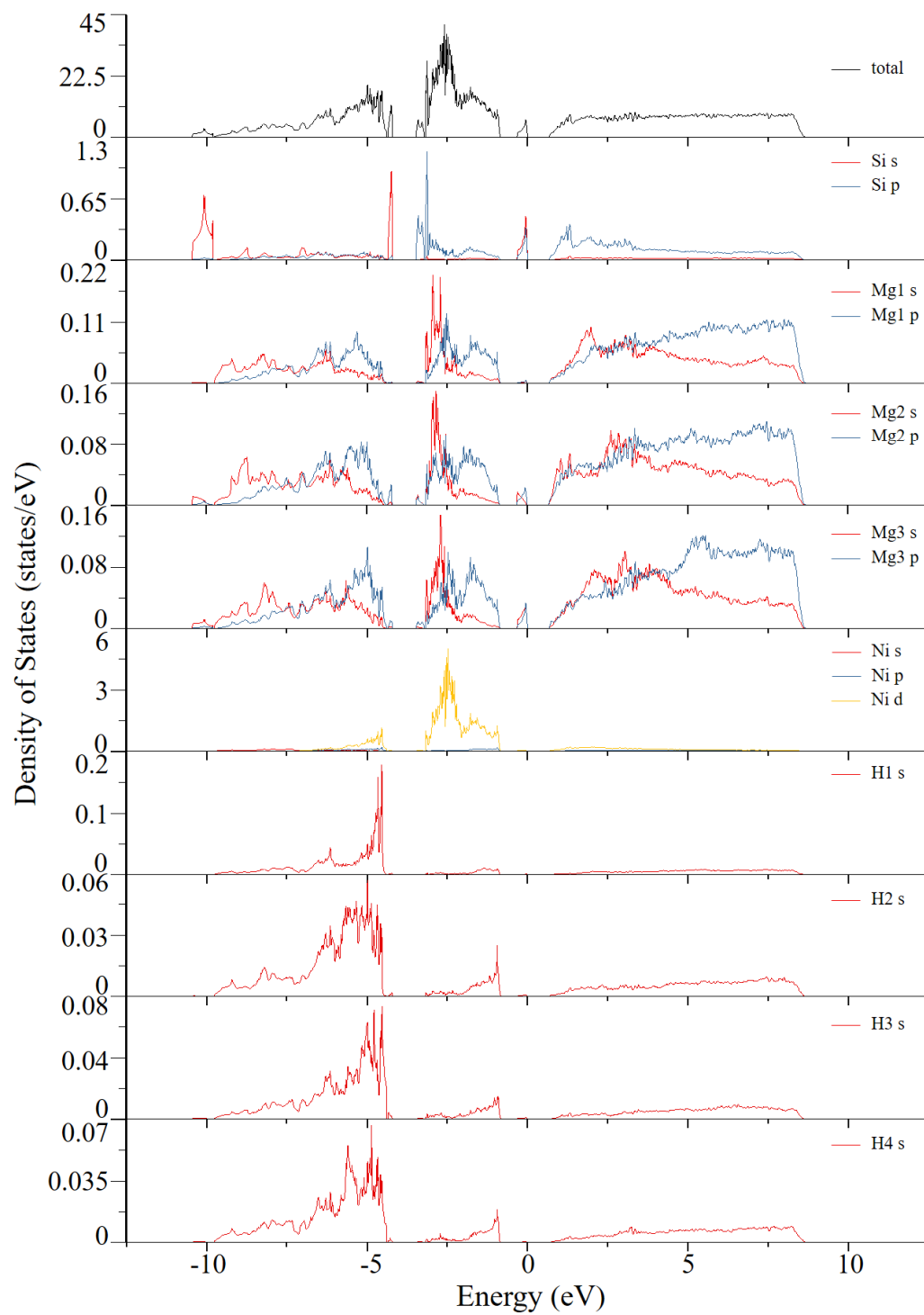


Figure 8. The calculated total and partial electronic DOS for the Si-doped system. The Fermi level is set at zero.

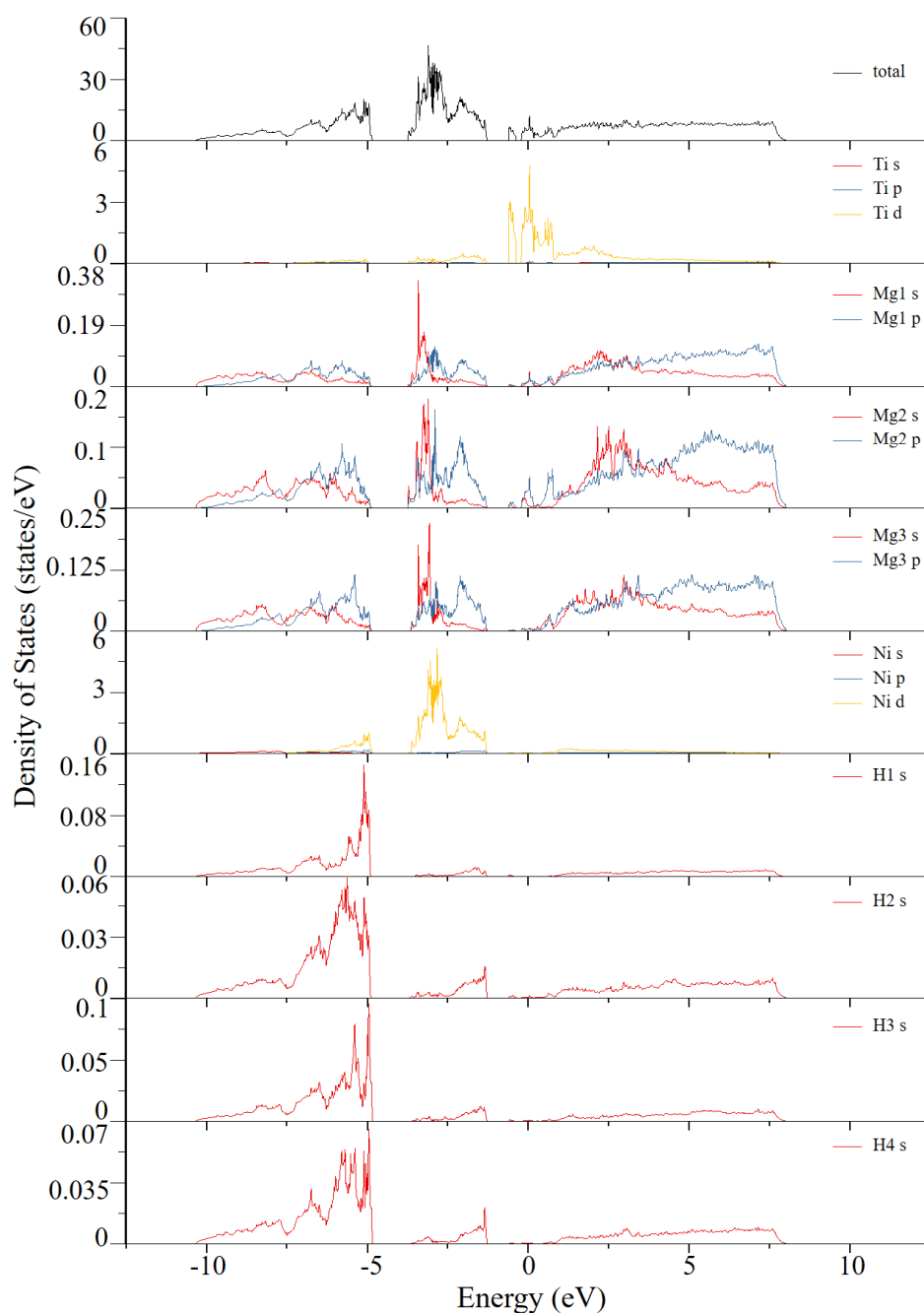


Figure 9. The calculated total and partial electronic DOS for the Ti-doped system. The Fermi level is set at zero.

4. Summary and Outlook

To conclude, we have screened nine kinds of elements for the doping of Mg_2NiH_4 as conversion electrode materials for lithium storage using the first-principles method. Through comparing the formation energy of doping, we first determined the most thermodynamically stable doping sites for each doping element. The electrochemical properties of nine doped materials, such as specific capacity, volume change, average voltage and band gap are theoretically predicted, in which we choose the three most promising elements (Na, Si and Ti) for doping to improve the electrochemical properties of the pristine Mg_2NiH_4 . Based on the three different doped crystal structures by Na, Si and Ti, we have further revealed their electronic structures. This theoretical study has important significance for the advancement of metal hydrides for lithium storage applications and is proposed to guide the

experimentalists in related areas to design and synthesize the conversion electrode materials with better properties.

Author Contributions: Conceptualization, Z.Q.; methodology, Z.Q. and G.J.; formal analysis, Z.Q. and G.J.; data curation, Z.Q., G.J., Y.R. and X.N.; writing—original draft preparation, Z.Q. and G.J.; writing—review and editing, Z.Q. and R.A.; project administration, Z.Q.; funding acquisition, Z.Q.

Funding: This research was funded by the Natural Science Foundation of China (51801113), the Natural Science Foundation of Shandong Province (ZR2018MEM001), and the Natural Science Foundation of Guangdong Province (2018A030313818). R.A. thanks the Swedish Research Council (VR) and Swedish Supercomputer facility (SNIC) for support.

Acknowledgments: Some scientific calculations in this work have been done on the HPC Cloud Platform of Shandong University.

Conflicts of Interest: The authors declare no conflict of interest.

References

1. Armand, M.; Tarascon, J.-M. Building better batteries. *Nature* **2008**, *451*, 652–657. [[CrossRef](#)]
2. Nitta, N.; Wu, F.X.; Lee, J.-T.; Yushin, G. Li-ion battery materials: Present and future. *Mater. Today* **2015**, *18*, 252–264. [[CrossRef](#)]
3. Yoon, G.; Kim, D.-H.; Park, I.; Chang, D.H.; Kim, B.; Lee, B.; Oh, K.; Kang, K. Using First-Principles Calculations for the Advancement of materials for Rechargeable Batteries. *Adv. Funct. Mater.* **2017**, *27*, 1702887. [[CrossRef](#)]
4. Lu, K.; Hu, Z.Y.; Ma, J.Z.; Ma, H.Y.; Dai, L.M.; Zhang, J.T. A rechargeable iodine-carbon battery that exploits ion intercalation and iodine redox chemistry. *Nat. Commun.* **2017**, *8*, 527. [[CrossRef](#)]
5. Urban, A.; Seo, D.-H.; Ceder, G. Computational understanding of Li-ion batteries. *NPJ Comput. Mater.* **2016**, *2*, 16002. [[CrossRef](#)]
6. Oumellal, Y.; Rougier, A.; Nazri, G.A.; Tarascon, J.-M.; Aymard, L. Metal hydrides for lithium-ion batteries. *Nat. Mater.* **2008**, *7*, 916–921. [[CrossRef](#)]
7. Qian, Z.; Sarkar, A.D.; Maark, T.A.; Jiang, X.; Deshpande, M.D.; Bououdina, M.; Ahuja, R. Pure and Li-doped NiTiH: Potential anode materials for Li-in rechargeable batteries. *Appl. Phys. Lett.* **2013**, *103*, 033902. [[CrossRef](#)]
8. Qian, Z.; Jiang, X.; Sarkar, A.D.; Maark, T.A.; Deshpande, M.D.; Bououdina, M.; Johansson, B.; Ahuja, R. Screen study of light-metal and transition-metal-doped NiTiH hydrides as Li-ion battery anode materials. *Solid State Ion.* **2014**, *258*, 88–91. [[CrossRef](#)]
9. Aymard, L.; Oumellal, Y.; Bonnet, J. Metal hydrides: An innovative and challenging conversion reaction anode for lithium-ion batteries. *Beilstein J. Nanotechnol.* **2015**, *6*, 1821–1839. [[CrossRef](#)]
10. Zhao, T.; Wang, Q.; Jena, P. Cluster-Inspired Design of Hige-Capacity Anode for Li-Ion Batteries. *ACS Energy Lett.* **2016**, *1*, 202–208. [[CrossRef](#)]
11. Liu, J.; Pang, W.K.; Zhou, T.; Chen, L.; Wang, Y.; Peterson, V.K.; Yang, Z.; Guo, Z.; Xia, Y. Li₂TiSiO₅: A low potential and large capacity Ti-based anode material for Li-ion batteries. *Energy Environ. Sci.* **2017**, *10*, 1456–1464. [[CrossRef](#)]
12. Oumellal, Y.; Rougier, A.; Tarascon, J.M.; Aymard, L. 2LiH + M (M = Mg, Ti): New concept of negative electrode for rechargeable lithium-ion batteries. *J. Power Sources* **2009**, *192*, 698–702. [[CrossRef](#)]
13. Mahata, A.; Bhauriyal, P.; Rawat, K.S.; Pathak, B. Pt₃Ti (Ti₁₉@Pt₆₀)-Based Cuboctahedral Core-Shell Nanocluster Favors a Direct over Indirect Oxygen Reduction Reaction. *ACS Energy Lett.* **2016**, *1*, 797–805. [[CrossRef](#)]
14. Jasen, P.V.; González, E.A.; Brizuela, G.; Nagel, O.A.; González, G.A.; Juan, A. A theoretical study of the electronic structure and bonding of the monoclinic phase of Mg₂NiH₄. *Int. J. Hydrog. Energy* **2007**, *32*, 4943–4948. [[CrossRef](#)]
15. Häussermann, U.; Blomqvist, H.; Noréus, D. Bonding and stability of the hydrogen storage material Mg₂NiH₄. *Inorg. Chem.* **2002**, *41*, 3684–3692. [[CrossRef](#)]
16. Wu, Z.; Zhu, L.; Yang, F.; Jiang, Z.; Zhang, Z. Influences of interstitial nitrogen with high electronegativity on structure and hydrogen storage properties of Mg-based metal hydride: A theoretical study. *Int. J. Hydrog. Energy* **2016**, *41*, 18550–18561. [[CrossRef](#)]

17. Martínez-Coronado, R.; Retuerto, M.; Torres, B.; Martínez-Lope, M.J.; Fernández-Díaz, M.T.; Alonso, J.A. High-pressure synthesis, crystal structure and cyclability of the Mg_2NiH_4 hydride. *Int. J. Hydrog. Energy* **2013**, *38*, 5738–5745. [[CrossRef](#)]
18. Zhang, J.; Zhou, D.W.; He, L.P.; Peng, P.; Liu, J.S. First-principles investigation of Mg_2Ni phase and high/low temperature Mg_2NiH_4 complex hydrides. *J. Phys. Chem. Solids* **2008**, *70*, 32–39. [[CrossRef](#)]
19. Orimo, S.; Züttel, A.; Ikeda, K.; Saruki, S.; Fukunaga, T.; Fujii, H.; Schlapbach, L. Hydriding properties of the MgNi-based systems. *J. Alloy. Compd.* **1999**, *293*, 437–442. [[CrossRef](#)]
20. Yvon, K.; Schefer, J.; Stucki, F. Structural studies of the hydrogen storage material Mg_2NiH_4 . 1. Cubic high-temperature structure. *Inorg. Chem.* **1980**, *20*, 2776–2778. [[CrossRef](#)]
21. Mitov, M.; Chorbadzhiyska, E.; Nalbandian, L.; Hubenova, Y. Nickel-based electrodeposits as potential cathode catalysts for hydrogen production by microbial electrolysis. *J. Power Sources* **2017**, *356*, 467–472. [[CrossRef](#)]
22. Hohenberg, P.; Kohn, W. Inhomogeneous electron gas. *Phys. Rev.* **1964**, *11*, B864. [[CrossRef](#)]
23. Blöchl, P.E. Projector augmented-wave method. *Phys. Rev. B* **1994**, *50*, 17953. [[CrossRef](#)]
24. Perdew, J.P.; Burke, K.; Ernzerhof, M. Generalized gradient approximation made simple. *Phys. Rev. Lett.* **1996**, *77*, 3865–3868. [[CrossRef](#)]
25. Nisar, J.; Pathak, B.; Ahuja, R. Screened hybrid density functional study on $\text{Sr}_2\text{Nb}_2\text{O}_7$ for visible light photocatalysis. *Appl. Phys. Lett.* **2012**, *100*, 181903. [[CrossRef](#)]
26. Cui, X.Y.; Medvedeva, J.E.; Delley, B.; Freeman, A.J.; Newman, N.; Stampfl, C. Role of embedded clustering in dilute magnetic semiconductors: Cr doped GaN. *Phys. Rev. Lett.* **2005**, *95*, 256404. [[CrossRef](#)]
27. Jiang, G.; Qian, Z.; Bououdina, M.; Ahuja, R.; Liu, X. Exploring pristine and Li-doped Mg_2NiH_4 compounds with potential lithium-storage properties: Ab initio insight. *J. Alloy. Compd.* **2018**, *746*, 140–146. [[CrossRef](#)]
28. Ceder, G.; Aydinol, M.K.; Kohan, A.F. Application of first-principles calculations to the design of rechargeable Li-batteries. *Comput. Mater. Sci.* **1997**, *8*, 161–169. [[CrossRef](#)]



© 2019 by the authors. Licensee MDPI, Basel, Switzerland. This article is an open access article distributed under the terms and conditions of the Creative Commons Attribution (CC BY) license (<http://creativecommons.org/licenses/by/4.0/>).